From Bloch Oscillations to Many Body Localization in Clean Interacting Systems

Evert P. L. van Nieuwenburg,[1,*] Yuval Baum,[1,*] and Gil Refael[1]

[1]*Institute of Quantum Information and Matter, California Institute of Technology, Pasadena, California 91125, USA*

In this work we demonstrate that non-random mechanisms that lead to single-particle localization may also lead to many-body localization, even in the absence of disorder. In particular, we consider interacting spins and fermions in the presence of a linear potential. In the non-interacting limit, these models show the well known Wannier-Stark localization. We analyze the fate of this localization in the presence of interactions. Remarkably, we find that beyond a critical value of the potential gradient, these models exhibit non-ergodic behavior as indicated by their spectral and dynamical properties. These models, therefore, constitute a new class of generic non-random models that fail to thermalize. As such, they suggest new directions for experimentally exploring and understanding the phenomena of many-body localization. We supplement our work by showing that by employing machine learning techniques, the level statistics of a system may be calculated without generating and diagonalizing the Hamiltonian, which allows a generation of large statistics.

I. INTRODUCTION

Since the phenomenon of many-body-localization (MBL) was re-postulated more than a decade ago [1–3], it has attracted a great deal of attention. It provides the first and only example of a generic quantum many-body system that cannot reach thermal equilibrium [4–10]. In recent years, an enormous theoretical effort was invested in understanding the nature of the MBL transition [11–13], the dynamical [14–16] and entanglement [17–21] properties of these systems and their response to external probes [22, 23] and periodic drives [24–28]. Also the experimental community [29–33] has found interest in this field, in particular, because these systems have the potential of storing information about initial states for long times, and hence may implement quantum memory devices. These systems may also be useful for dynamical quantum control, as they allow the application of driving protocols without heating the system to an infinite temperature.

A key ingredient for achieving the MBL phase is disorder (randomness). The roots of this phase lie within the phenomenon of Anderson localization [1], where non-interacting particles form a localized non-ergodic phase. Questioning the fate of Anderson localization in the presence of interactions led to the discovery of the MBL phase.

We attempt to go beyond the conventional paradigm of MBL, and ask whether randomness is indeed an essential ingredient in achieving generic non-ergodic interacting phases. Viewing MBL as a competition between single-particle localization and interactions, one may wonder whether a localizing mechanism that does not require disorder may produce similar results. It was suggested that quasi-many-body localization may exist in a translationally invariant quantum disentangled liquid, where light particles evade thermalization (for long times) by localizing on heavy particles [34, 35]. Moreover, it was shown that clean 1D systems with quasi-periodic potentials may host an MBL phase [36, 37]. The model we propose in this work respects the crystal symmetry exactly, and hence, in that regard it is the first example of a truly discrete translational invariant model that supports the MBL phase.

A well known mechanism for localizing single particles is the Wannier-Stark effect [38], in which particles living on a lattice become localized in the presence of a linear potential. We refer to this phenomenon as Bloch localization. Notice that beside lacking randomness, such systems also preserve translation-invariance as the linear potential represents a uniform force and may be replaced by a time-dependent vector potential. The interplay between interactions and linear fields has been investigated in the past. It was shown that the oscillatory part of the current, i.e. Bloch oscillations (BO), decays as the interaction strength increases [39–41]. It was also shown that the presence of a uniform force changes the nature of the evolution of an initial state under the non-linear Schrödinger equation (NLSE) as the non-linearity increases, e.g., for a large non-linearity the dynamics is localized. Yet, the ergodic properties and the generality (stability) of these phases can not be inferred from these works. The absence of BO does not necessarily signify ergodicity and the dynamics of generic interacting models can not be captured by the NLSE, which is generally valid only as a mean field description of weakly interacting Bosons [42]. Moreover, only the evolution of low energy (near ground state) states have been considered and the stability of the above phenomenon was not analyzed. In this work, we propose the idea that the essential ingredient for MBL is single-particle-localization, which does not necessarily require disorder. We analyze the spectral and the dynamical properties of one-dimensional interacting fermions and spins in the presence of both disorder and a linear potential. We show that by considering these two different localizing mechanisms, i.e., disorder (W) and linear fields (F), one may construct a two-dimensional phase diagram in the (F, W)-space which hosts a connected non-ergodic (MBL) phase. We find that above a critical value F_c, the MBL phase extends down to the

* These two authors contributed equally.

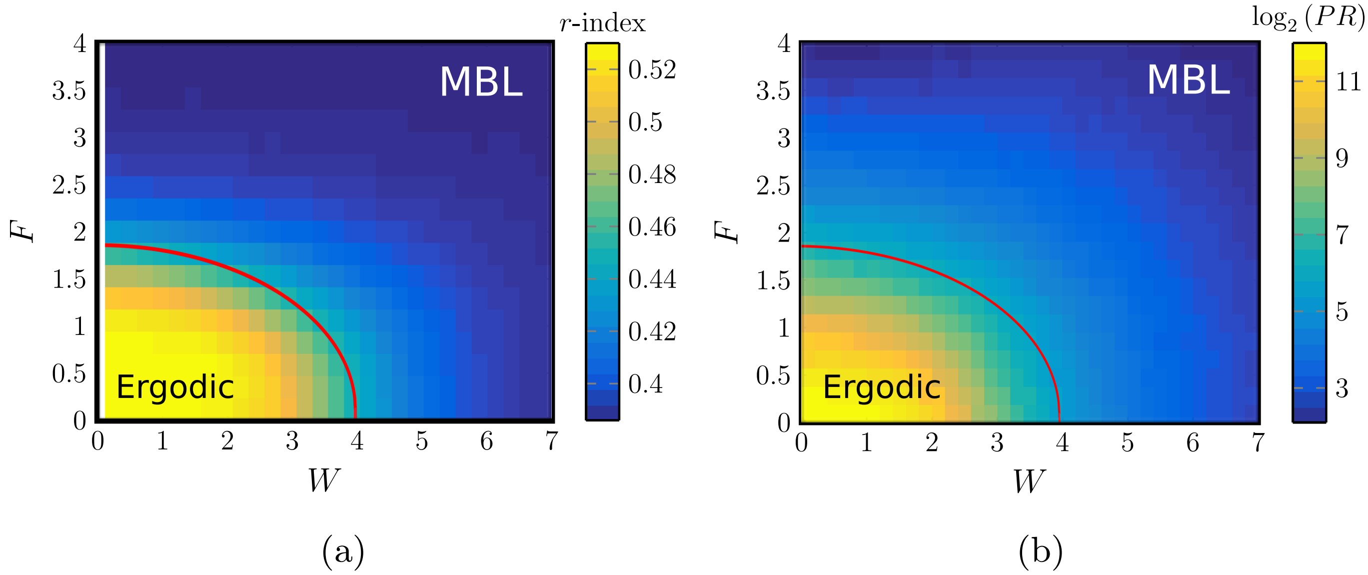

FIG. 1. These plots constitute the main results of the paper and demonstrate the existence of a potential-gradient induced MBL phase. (a) The r-index as a function of disorder and field strength as calculated for the Hamiltonian in Eq. (6) with $L = 16$ and $J_0 = J_z = 1$ (averaged over 125 realizations). Evidently, a phase boundary exists between a region with $r = 0.53$ (Wigner-Dyson) for small values of W and F (the ergodic dome) to a region with $r = 0.386$ (Poisson). (b) The averaged participation ratio ($PR = 1/IPR$) as a function of disorder and field strength for the same system as in (a). Consistently with the level statistics, inside the ergodic dome the PR is proportional to the Hilbert space dimension ($\mathcal{D}$), while outside the dome it becomes small and independent of $\mathcal{D}$. Notice that in (b) the line $W = 0$ is included in the data. In both cases the red line serves only as a guide to eye and is a contour or $r \approx 0.46$.

clean limit, i.e., the $W = 0$ line.

It is worth mentioning that integrable models, such as the 1D Heisenberg and transverse field Ising models, are known examples of clean models that fail to thermalize. While these models fail to thermalize, they are sensitive to the existence of small integrability-breaking terms such as disorder or longer range interactions and hopping. In this sense the model we suggest is more generic, since the addition of disorder and/or weak longer range hopping and interactions does not lead to thermalization.

The existence of generic clean models that fail to thermalize may have important implications both theoretically and experimentally. From the theory side, it can simplify dramatically the numerical effort in analyzing these interacting systems. Moreover, the lack of randomness gives hope that the nature of the MBL transition, the emergent conserved quantities and the generalization to higher dimensions may be approached analytically. From the experimental side the necessity of strong disorder is a major drawback. In intrinsic systems it is not clear whether such strong disorder generically exists. In controlled systems, such as optical lattices, only quasi-random disorder or correlated disorder, e.g. speckle potentials, may be implemented and a repetition over many realizations is needed due to the small size of the systems [43, 44]. In stark contrast, linear field (tilt in optical lattices) may be implemented relatively easily and it provides the ability to experimentally realize these systems in a highly reproducible way, and without the necessity of many repetitions. Unlike integrable models, the inevitable existence of unwanted terms such as weak disorder, should not have a dramatic effect on the dynamics.

II. BACKGROUND AND MODEL DEFINITION

A. Bloch localization

Our ultimate goal is to understand the fate of Bloch localization in the presence of interactions. In this section we briefly review the properties of non-interacting particles in the presence of a uniform force (linear potential). Consider a 1D lattice model in the presence of a linear potential,

$$H_0 = \sum_j t(c_j^\dagger c_{j+1} + h.c) - Fjc_j^\dagger c_j, \tag{1}$$

where c_j annihilates a particle from lattice site j, t is the nearest neighbor hopping amplitude, and F is the uniform force. The Hamiltonian can be diagonalized by the following transformation,

$$c_j = \sum_m \mathcal{J}_{m-j}\left(x\right) b_m, \tag{2}$$

with $\mathcal{J}_n$ being the Bessel functions of the first kind and $x = 2t/F$. Under this transformation Eq. (1) becomes,

$$H_0 = -\sum_m Fm\, b_m^\dagger b_m. \tag{3}$$

Overall, the spectrum contains a ladder of equally spaced levels where, by inverting Eq. (2), an eigenstate with energy Fm is given by,

$$b_m = \sum_j \mathcal{J}_{j-m}(x)\, c_j. \tag{4}$$

Since $|\mathcal{J}_n(x)| < e^{-|n|}$ for $x \ll n$, all the eigenstates are localized for any $F \neq 0$. Each eigenstate, $b_m^\dagger|vac\rangle$, is localized around site m with an inverse localization length given by $\xi^{-1} \approx 2\sinh^{-1}(1/x)$.

Unlike for Anderson localization, where the localization length is energy dependent (smaller near the middle of the energy band), for Bloch localization case the localization length is an energy independent quantity. Another prominent difference between the two is the form of the density of states, where in the case of Bloch localization the spectrum forms an ordered ladder even deep in the localized phase.

B. Model Definition

The basic model we wish to analyze concerns the interplay between the two mechanisms of single particle localization (disorder and linear field) and interactions. For that, we consider a 1D lattice of interacting spinless fermions in the presence of disorder and a uniform force,

$$H = \sum_j t(c_j^\dagger c_{j+1} + h.c) - Fjn_j + h_j n_j + U n_j n_{j+1}, \tag{5}$$

where c_j annihilates a particle from lattice site j, $n_j = c_j^\dagger c_j$ is the density, t is the nearest-neighbor (nn) hopping amplitude, F is the uniform force, $h_j \in [-W, W]$ is a random on-site potential with strength W and U is the nn interaction strength.

The above fermionic Hamiltonian may be mapped, via a Jordan-Wigner transformation, into an equivalent spin-1/2 chain (Heisenberg),

$$H = \sum_j J_0(S_j^x S_{j+1}^x + S_j^y S_{j+1}^y) + J_z S_j^z S_{j+1}^z + FjS_j^z + h_j S_j^z, \tag{6}$$

with $J_0 = 2t$ and $J_z = U$ while F and $h_j \in [-W, W]$ defined as before. In the rest of this paper we will analyze the localization and dynamical properties of these Hamiltonians as a function of the interaction strength, force and disorder strength. Since the particle-number (fermionic model) or the total S_z (spin model) are conserved, we focus our analysis on the half-filled ($S_z = 0$) sector. Regardless, the results do not depend much on the specific sector.

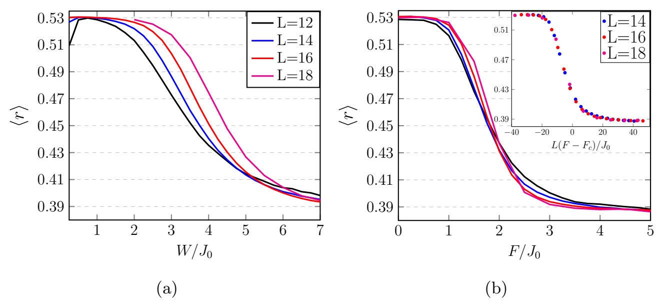

FIG. 2. The r-index as calculated for the Hamiltonian in Eq. (6) with $J_0 = J_z = 1$ for different system sizes, $L = 12, 14, 16, 18$. In (a) the r-index is plotted as a function of W for zero linear field. In (b) the r-index is plotted as a function of F for a fixed disorder strength $W = 0.5$, where in the inset we plotted the data as a function of $L(F - F_c)$ with $F_c = 2.2$.

III. RESULTS AND DISCUSSION

A. Level statistics

A well established signature for the transition from ergodic to non-ergodic dynamics is the level statistics of the many body spectrum. In particular, generic ergodic Hamiltonians belong to the Gaussian Orthogonal Ensemble (GOE) [45–47] and their level-spacings, $\delta_n = \epsilon_{n+1} - \epsilon_n$, obey the Wigner-Dyson distribution. On the other hand, for non-ergodic systems the level-spacings obey the Poisson distribution. Both distributions are often characterized by a single parameter, $r = \langle \min(\delta_n, \delta_{n+1}) / \max(\delta_n, \delta_{n+1}) \rangle$, which conveniently avoids the need for unfolding the spectrum. For the Wigner-Dyson distribution $r \approx 0.530$ and $r = \ln 4 - 1 \approx 0.386$ for the Poisson distribution.

We diagonalize the Hamiltonian in Eq. (6) for $L = 12, 14, 16, 18$ spins using exact diagonalization, with $J_0 = J_z = 1$ and for different values of F and W. In appendix A we show that by employing machine learning techniques, statistics for the r-value may be generated from h_j directly without the need of diagonalizing the Hamiltonian.

In Fig. 1(a) we show the r value (averaged over different disorder realizations) in the space of (F, W). We find that the ergodic phase lives in a dome-shaped region near the origin of the (F, W) space. The line $F = 0$ corresponds to the often discussed MBL transition near the critical disorder strength W_c. As F increases, the value of W_c decreases. Above a critical value of F, the critical disorder appears to go to zero and the non-ergodic phase appears also in the clean non-disordered limit.

In Fig. 2 we show the r value for different system sizes as a function disorder (zero field) and as a function of the field (for a fixed weak disorder). The critical values may be extracted by finite size scaling through a scaling collapse. The case of zero field was analyzed in several works [11, 48–50] in which the critical disorder was found to be in the range $W_c \sim 7.5 \pm 0.5$ (notice a possible factor of 2 due to a different definition of the spin matrices). For the weak disorder case we plot the data, Fig. 2 (inset), as a function of $L^{1/\nu}(F - F_c)$. We find that the critical exponent is $\nu \approx 1$ and the critical field is $F_c \approx 2.2$, for which the data collapse on one curve. In appendix B we provide more details regarding the finite size scaling. In appendix C we show that the above results are not sensitive to integrability-breaking terms such as next-next-nearest-neighbor hopping and interactions.

Notice that in this part, we always considered $W > 0.2$, since for small enough disorder, small systems behave as clean systems which leads to symmetry related degeneracies in the spectrum.

B. Inverse participation ratio

Analyzing level statistics of clean systems requires a separation of the Hilbert space into momentum sectors, since degeneracies due to symmetries have to be removed. For finite systems and below a critical disorder strength, the system behaves similar to a clean system. Therefore, the level statistics becomes a less reliable measure for small disorder strengths since degeneracies start to appear due to the emergence of translation symmetry. A quantity which is less sensitive to symmetries is the inverse participation ratio (IPR). The IPR is also a measure of the long-time return probability of arbitrary initial states. To see that, consider the return probability of a state $|\psi_0\rangle$,

$$P(t) = \left|\langle\psi_0|\hat{U}(t)|\psi_0\rangle\right|^2, \tag{7}$$

where $\hat{U}(t)$ is the time evolution operator. The state $|\psi_0\rangle$ may be expanded in terms of the Hamiltonian eigenstates, $|\psi_0\rangle = \sum_n c_n|\phi_n\rangle$. Eq. (7) becomes,

$$P(t) = \sum_{n,m} |c_n|^2|c_m|^2 e^{-\mathrm{i}(\epsilon_n - \epsilon_m)t}. \tag{8}$$

The IPR is obtained as the long-time limit of the return probability,

$$IPR = \lim_{T\to\infty} \frac{1}{T}\int_0^T dt P(t) = \sum_{n,m} |c_n|^2|c_m|^2 \delta_{\epsilon_n,\epsilon_m}. \tag{9}$$

In the absence of degeneracies, Eq. (9) becomes $IPR = \sum_n |c_n|^4$. Clearly, if the initial state is an eigenstate then $IPR = 1$, while if the initial states is an equal-superposition of all the eigenstates then $IPR = 1/\mathcal{D}$, where $\mathcal{D}$ is the Hilbert space dimension which generically is exponential in the system size. In the following we average the IPR over different initial states which we choose to be eigenstates of some local operators, e.g., s^z_j. For ergodic systems, the IPR should be exponentially small in the system size and the system should lose its memory of the initial state. In stark contrast, in the localized phase the IPR converges to a positive system size independent constant.

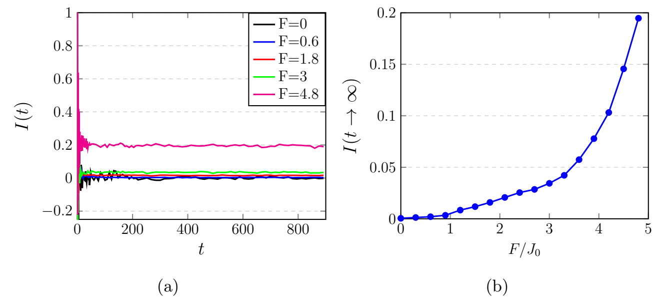

FIG. 3. (a) The imbalance as a function of time for different field strength and for fixed weak disorder $W = 0.2$, where $L = 14$, $J_z = J_0 = 1$. (b) The long time limit of the imbalance as a function of the field. Below a critical value $F \lesssim F_c$ the long time limit of I tends to zero, while above that value the long time limit tends to a finite value that increases with the field.

In Fig. 1(a) we present the averaged and normalized participation ratio, $\langle PR\rangle = \mathcal{D}/IPR$, in the space of (F, W). While the IPR is a smooth function, there is a clear transition between a region where the IPR is exponentially small to a region where the IPR is independent of system size. These regions agree with the results obtained in the previous section. Here also the line $W = 0$ behaves in a similar way (c.f. Fig. 1(b)), where the IPR becomes independent of system size as a function of F.

C. Dynamics and experimental measurables

The distinction between ergodic and non-ergodic dynamics is well-captured by the level-statistics and the participation ratio. Yet both these measures are hard to access in experiments. As shown in Refs. 30, 31, and 33, the nature of the dynamics is examined by tracking the dynamics of an initially prepared out-of-equilibrium density configuration. We numerically show that the existence of a linear field prevents thermalization. For concreteness, we consider a similar out-of-equilibrium initial state as in Ref. 30. The system is prepared in a anti-ferromagnetic configuration (or charge density wave for the fermions), where the spins on odd sites point down (empty) and on even sites point up (full). We then track the time evolution of the odd-even imbalance, $I = (S^e_{z,\uparrow} - S^o_{z,\uparrow})/(S^o_{z,\uparrow} + S^e_{z,\uparrow})$.

In ergodic systems, I is expected to decay to zero with a typical relaxation time τ. We show that while indeed this is the case when the linear field is small, both for the clean case and for weak disorder, beyond a critical field strength, the long time limit of I is different from zero. In Fig. 3(a) we show the imbalance I in a system of 16 spins (sites) as a function of time for different values of the field

F and for a fixed weak disorder strength ($W = 0.2$). In Fig. 3(b) we show the long time limit as a function of F. Below a critical value $F \lesssim F_c$ the long time limit of I tends to zero, while above that value the long time limit tends to a finite value that increases with the field.

IV. MBL IN TWO-DIMENSIONS

Dimensionality plays a crucial role in the localization properties of single particles in the presence of disorder. As a result, the lesson we learned about the effect of interaction on the Anderson localized (AL) phase in 1D can not be trivially extended to higher dimensions. Indeed, the nature, and even the existence, of a many-body-localized phase in $D > 1$ is a hotly debated subject. While theoretical works [51–53] argue that a true MBL phase does not exist, experimental works [30, 32, 33] have shown indications for such a phase in $D > 1$.

Similar questions may be posed in the context of the uniform field as a cause for single particle localization. In stark contrast to the AL phase, this phase is less sensitive to dimensionality. In particular, if the the force $\mathbf{F}$ has a finite projection, F_i, on all lattice vectors, and the hopping amplitudes J_0 are identical for all directions, then all the eigenstates are localized in all directions with a localization length $\xi \propto J_0/F_i$. This similarity between $D = 1$ and $D > 1$, gives the hope that the 1D localization may be extended to higher dimensions as well.

In Fig. 4 we present the level statistics (r index) of a 2D Heisenberg model as a function of the uniform force $\mathbf{F} = F(\sqrt{2}, 1)$ and disorder. Similar to the 1D case, we see a clear transition from a Wigner-Dyson distribution to Poisson distribution. Since we are restricted to very small system sizes (4×4 lattice), we can not make a meaningful statement about the nature of this transition, however, we hope that these ideas will stimulate further works in this directions.

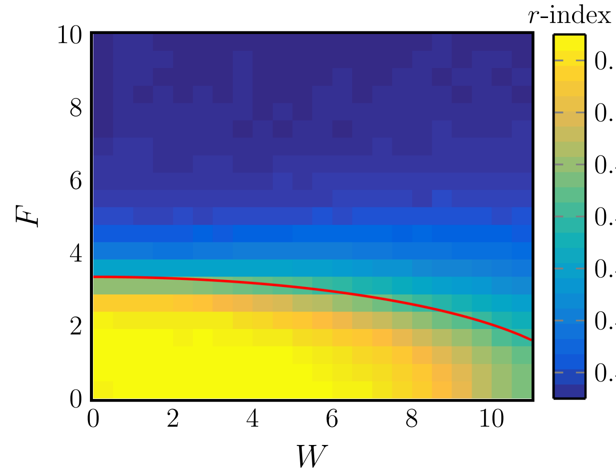

FIG. 4. The level statistics (r-value) as a function of the field strength, F, and disorder strength, W, for a disordered 2D system of 4×4 spins with an incommensurate force $\mathbf{F} = F(\sqrt{2}, 1)$ (averaged over 32 realizations). The red line is a guide to the eye and is given by a contour of $r \approx 0.46$.

V. CONCLUSIONS

In this work we analyzed the effect of interactions on single particle localization that arise both from disorder, W, and from the existence of linear potentials F. With that, we showed that the notion of a many-body localized (MBL) phase may be generalized also to a class of clean (non-integrable) systems. In particular, we find that a phase boundary in the space (F, W) exists, beyond which the resulting phase fails to thermalize. We find that, unlike in clean integrable models, this non-ergodic phase is stable to perturbations, and shares all the familiar fingerprints of the well studied MBL phase in the presence of disorder.

The existence of such a phase demonstrates that randomness is not an essential ingredient for the emergence of stable non-ergodic interacting phases. Such a conclusion may have a profound impact on the realization of these non-ergodic phases. Unlike disorder potentials, linear potentials are relatively easy to implement, both in cold atom and in solid-state setups, and are highly tunable and may be controlled dynamically. The ability to realize stable and generic non-ergodic phases is an important step toward the realization of quantum memory devices that may store information for long times. Moreover, the lack of randomness and the low sensitivity to dimensionality may render these systems more accessible to a further theoretical investigation, both numerically and analytically.

ACKNOWLEDGMENTS

E.v.N. gratefully acknowledges financial support from the Swiss National Science Foundation through grant P2EZP2-172185. G.R. is grateful to the ARO MURI W911NF-16-1-0361 "Quantum Materials by Design with Electromagnetic Excitation" sponsored by the U.S. Army as well as the Packard Foundation and for the hospitality of the Aspen Center for Physics, which is supported by National Science Foundation grant PHY-1607761, where part of the work was done. We are grateful for support from the IQIM, an NSF physics frontier center funded in part by the Moore Foundation.

Appendix A: Data augmentation using machine learning

The different disorder realizations we study in this manuscript differ only in the values for the on-site potentials. Given the on-site potentials, there exists a

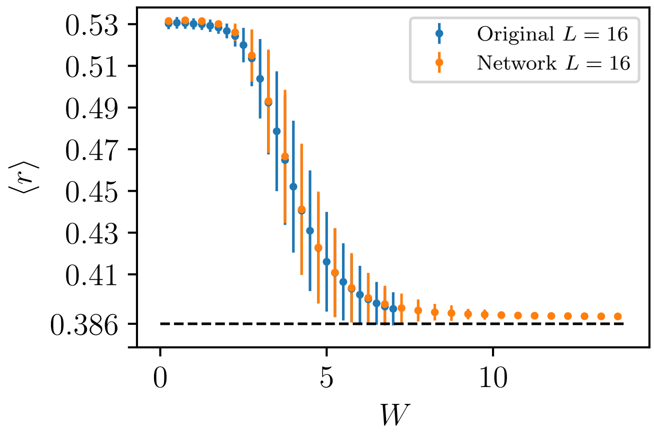

FIG. 5. The original $L = 16$ data and the machine learned map from the disorder realization h_1 through h_{16} to the resulting r-statistics. With the network we are able to generate considerably more realizations (10^6 versus 10^3) in a much shorter timespan, provided that the network is capable of learning and generalizing. The sigmoid output neuron rather than linear for optimizing the mean-squared-error ensures convergence of the output as a function of W. Error bars indicate the standard deviation over the number of realizations, and the black dashed horizontal line indicates the Poissonian r-value of $\ln 4 - 1$.

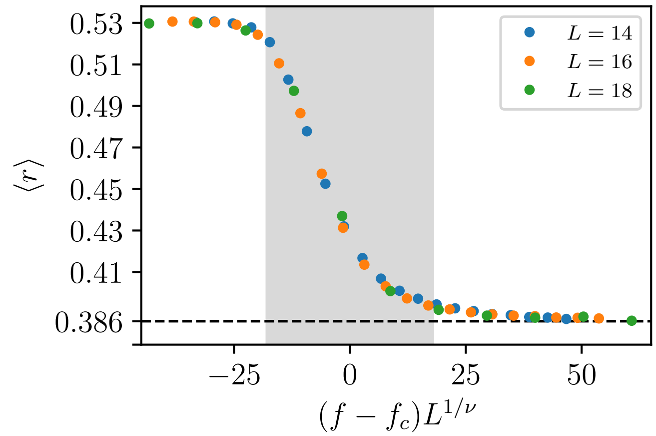

FIG. 6. Collapse of the $W = 0.5$ data for system sizes $L = 14, 16, 18$, as a function of the field strength f. The collapse is obtained by rescaling the fields according to $f \to (f - f_c)L^{1/\nu}$ with $f_c = 2.08$ and $\nu = 0.952$. The gray area indicates the width w that was used to make the curves collapse, and is the width at which the collapse is most stable against inclusion or removal of the $L = 12$ data.

procedure that results in the value for the r-statistics. Namely, one builds the corresponding Hamiltonian matrix and diagonalizes it to obtain the eigenvalues ϵ_n. The r-statistics is obtained by looking at neighboring eigenvalue differences $\delta_n = \epsilon_{n+1} - \epsilon_n$ and computing the ratio $r = \langle \min(\delta_n, \delta_{n+1}) / \max(\delta_n, \delta_{n+1}) \rangle$ as discussed in the main text.

Here, however, we ask whether or not a more direct (approximate) map exists from the on-site potentials to r. Rather than trying to explicitly construct it, we attempt to train a neural network to perform this map for us. Hence we generate a large data-set of pairs $(\mathbf{h}, r)$, where $\mathbf{h}$ is a vector of the on-site potentials augmented with the value of W from which they were drawn, and r is the resulting r-statistics for this particular realization. These serve as the input and output respectively for the machine learning model.

Provided that such a mapping exists and that the network is capable of learning it, the resulting network can be used to generate more r-values by using it to predict on more realizations. This allows one to generate statistics much faster compared to running the full exact diagonalization. It must be noted that this procedure cannot take away the inherent statistical uncertainty due to the finite size of the system. Particularly, for disorder strengths near the transitions point, the exact r-values of systems with different realizations drawn from the same distribution, lie within a relatively large window. As the system becomes larger this window becomes smaller. For example, already by including a few hundreds of realizations, for $L = 16$, the error bars near the transition are dominated by the intrinsic finite size effect and cannot be improved by adding more realizations.

In Fig. 5 we demonstrate the above procedure for the $L = 16$ data, for which the data-set consists of $\sim$ 15k entries (25 values of W spread over $\sim$ 550 realizations). We split off 10% of the data as a validation set, and train a network with the following architecture:

1. Two convolutional layers with 32 filters and kernel sizes 6 and 3, followed by a maximum pooling of size 3.

2. A convolutional layer with 64 filters and kernel size 2, followed by a global average pooling.

3. Two fully connected sigmoid layers with 256 and 128 neurons respectively, and dropout 0.5.

4. An output layer with a single sigmoid neuron.

We train the network with the Adam [54] optimizer to minimize the mean-squared-error loss function, and achieve a validation loss of $\sim 2 \cdot 10^{-5}$ in 100 epochs of batchsize 32. In our experiments, we have found no particular reason for the above network to work better than others, but we found that considerably simpler networks (e.g. just fully connected layers) converge much slower. For the purpose of extracting the mapping, our chosen network might be hard to interpret. It would be an interesting research direction however to see if the approximate mapping can be extracted from a network, or whether a single network can be trained on different system sizes to extract finite size behavior. Both would potentially allow predictions to be made on larger system sizes than trained on, although further investigation into this question is required.

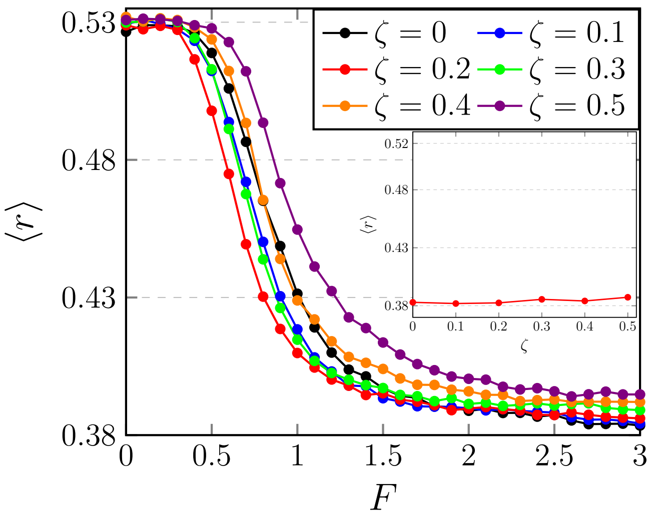

FIG. 7. The level statistics (r-index) as a function of the linear field for different values of the integrability-breaking strength, ζ. The calculation was done for a system of 14 sites (half-filled) with a fixed weak disorder $W = 0.2$ (averaged over 50 realizations),$t = 1/2$ and $U = 1$. Inset: the r-index of a clean system of 16 sites with fixed field $F = 3$ as a function of ζ.

Appendix B: Finite size scaling

In this appendix we discuss the transition from the ergodic to the non-ergodic phase as a function of the linear field f. To do so, we fix $W = 0.5$ and perform a finite size scaling analysis attempting to collapse the curves for different system sizes. We consider a universal function $g\left((f - f_c)\, L^{1/\nu}\right)$ for the r-statistics, and optimize the parameters f_c and ν so that the rescaled r-statistics curves for the different sizes collapse.

Each of the curves is first rescaled with proposed f_c and ν after which we use spline interpolation to numerically minimize the cost function $C(f_c, \nu) = \sum_{i<j} \int_x (y_i(x) - y_j(x))^2$, where i, j both run over system sizes $L = 12, 14, 16, 18$ and $y_i(x)$ represents the spline-interpolated data. The integration regime x is taken to be centered around the transition (i.e. $x = 0$) and has a width $2w$ that we vary to obtain statistics on f_c and ν. In the collapse including the system size $L = 12$ data, the $L = 12$ curve is consistently the most off. In the spirit of Ref. [48] we consider the width w for which the extracted parameters are least sensitive to the inclusion/removal of the $L = 12$ data. This results in the parameters $f_c = 2.08 \pm 0.10$ and $\nu = 0.952(5)$. The resulting collapse for this set of parameters is shown in Fig. 6.

Appendix C: sensitivity to integrability-breaking terms

We now consider an extended version of Eq. (5),

$$H = \sum_j t(c_j^\dagger c_{j+1} + h.c) - Fjn_j + h_j n_j + U n_j n_{j+1} + \zeta\left(c_j^\dagger c_{j+2} + h.c + n_j n_{j+2}\right). \tag{C1}$$

In the absence of both disorder and linear field, the above model is integrable for $\zeta = 0$. We show that also in the presence of the integrability-breaking terms, the application of linear field (with or without disorder) leads to a transition from a Wigner-Dyson level statistics (ergodic) to a Poisson level statistics (non-ergodic). While the value of the critical field depends on ζ and the disorder strength, the qualitative behavior is indifferent to these terms. In Fig. 7 we show the r-index as a function of the linear field strength. Different curves represent different values of ζ.

[1] P. W. Anderson, "Absence of diffusion in certain random lattices," Phys. Rev. **109**, 1492–1505 (1958).
[2] D.M. Basko, I.L. Aleiner, and B.L. Altshuler, "Metalinsulator transition in a weakly interacting many-electron system with localized single-particle states," Annals of Physics **321**, 1126 – 1205 (2006).
[3] I. V. Gornyi, A. D. Mirlin, and D. G. Polyakov, "Interacting electrons in disordered wires: Anderson localization and low-t transport," Phys. Rev. Lett. **95**, 206603 (2005).
[4] Rahul Nandkishore and David A. Huse, "Many-body localization and thermalization in quantum statistical mechanics," Annual Review of Condensed Matter Physics **6**, 15–38 (2015).
[5] Dmitry A. Abanin and Zlatko Papi, "Recent progress in many-body localization," Annalen der Physik **529**, 1700169–n/a (2017), 1700169.
[6] John Z. Imbrie, "Diagonalization and many-body localization for a disordered quantum spin chain," Phys. Rev. Lett. **117**, 027201 (2016).
[7] Maksym Serbyn, Z. Papić, and Dmitry A. Abanin, "Local conservation laws and the structure of the many-body localized states," Phys. Rev. Lett. **111**, 127201 (2013).
[8] David A. Huse, Rahul Nandkishore, and Vadim Oganesyan, "Phenomenology of fully many-body-localized systems," Phys. Rev. B **90**, 174202 (2014).
[9] V. Ros, M. Mller, and A. Scardicchio, "Integrals of motion in the many-body localized phase," Nuclear Physics B **891**, 420 – 465 (2015).
[10] Anushya Chandran, Isaac H. Kim, Guifre Vidal, and Dmitry A. Abanin, "Constructing local integrals of motion in the many-body localized phase," Phys. Rev. B **91**, 085425 (2015).
[11] Vadim Oganesyan and David A. Huse, "Localization of interacting fermions at high temperature," Phys. Rev. B **75**, 155111 (2007).
[12] Arijeet Pal and David A. Huse, "Many-body localization phase transition," Phys. Rev. B **82**, 174411 (2010).

[13] Ronen Vosk, David A. Huse, and Ehud Altman, "Theory of the many-body localization transition in one-dimensional systems," Phys. Rev. X **5**, 031032 (2015).

[14] Yevgeny Bar Lev and David R. Reichman, "Dynamics of many-body localization," Phys. Rev. B **89**, 220201 (2014).

[15] Christopher David White, Michael Zaletel, Roger S. K. Mong, and Gil Refael, "Quantum dynamics of thermalizing systems," Phys. Rev. B **97**, 035127 (2018).

[16] E. van Nieuwenburg, E. Bairey, and G. Refael, "Learning phase transitions from dynamics," ArXiv e-prints (2017), arXiv:1712.00450 [cond-mat.dis-nn].

[17] Bela Bauer and Chetan Nayak, "Area laws in a many-body localized state and its implications for topological order," Journal of Statistical Mechanics: Theory and Experiment **2013**, P09005 (2013).

[18] Marko Žnidarič, Toma ž Prosen, and Peter Prelovšek, "Many-body localization in the heisenberg xxz magnet in a random field," Phys. Rev. B **77**, 064426 (2008).

[19] Jens H. Bardarson, Frank Pollmann, and Joel E. Moore, "Unbounded growth of entanglement in models of many-body localization," Phys. Rev. Lett. **109**, 017202 (2012).

[20] Vedika Khemani, S. P. Lim, D. N. Sheng, and David A. Huse, "Critical properties of the many-body localization transition," Phys. Rev. X **7**, 021013 (2017).

[21] Zhi-Cheng Yang, Alioscia Hamma, Salvatore M. Giampaolo, Eduardo R. Mucciolo, and Claudio Chamon, "Entanglement complexity in quantum many-body dynamics, thermalization, and localization," Phys. Rev. B **96**, 020408 (2017).

[22] Sarang Gopalakrishnan, Markus Müller, Vedika Khemani, Michael Knap, Eugene Demler, and David A. Huse, "Low-frequency conductivity in many-body localized systems," Phys. Rev. B **92**, 104202 (2015).

[23] Timothy C. Berkelbach and David R. Reichman, "Conductivity of disordered quantum lattice models at infinite temperature: Many-body localization," Phys. Rev. B **81**, 224429 (2010).

[24] Achilleas Lazarides, Arnab Das, and Roderich Moessner, "Fate of many-body localization under periodic driving," Phys. Rev. Lett. **115**, 030402 (2015).

[25] Luca D'Alessio and Marcos Rigol, "Long-time behavior of isolated periodically driven interacting lattice systems," Phys. Rev. X **4**, 041048 (2014).

[26] Luca DAlessio and Anatoli Polkovnikov, "Many-body energy localization transition in periodically driven systems," Annals of Physics **333**, 19 – 33 (2013).

[27] Vedika Khemani, Achilleas Lazarides, Roderich Moessner, and S. L. Sondhi, "Phase structure of driven quantum systems," Phys. Rev. Lett. **116**, 250401 (2016).

[28] Karthik Seetharam, Paraj Titum, Michael Kolodrubetz, and Gil Refael, "Absence of thermalization in finite isolated interacting floquet systems," Phys. Rev. B **97**, 014311 (2018).

[29] J. Smith, A. Lee, P. Richerme, B. Neyenhuis, P. W. Hess, P. Hauke, M. Heyl, D. A. Huse, and C. Monroe, "Many-body localization in a quantum simulator with programmable random disorder," Nature Phys. **12** (2016), 10.1038/nphys3783.

[30] Jae-yoon Choi, Sebastian Hild, Johannes Zeiher, Peter Schauß, Antonio Rubio-Abadal, Tarik Yefsah, Vedika Khemani, David A. Huse, Immanuel Bloch, and Christian Gross, "Exploring the many-body localization transition in two dimensions," Science **352**, 1547–1552 (2016).

[31] Michael Schreiber, Sean S. Hodgman, Pranjal Bordia, Henrik P. Lüschen, Mark H. Fischer, Ronen Vosk, Ehud Altman, Ulrich Schneider, and Immanuel Bloch, "Observation of many-body localization of interacting fermions in a quasirandom optical lattice," Science **349**, 842–845 (2015).

[32] S. S. Kondov, W. R. McGehee, W. Xu, and B. DeMarco, "Disorder-induced localization in a strongly correlated atomic hubbard gas," Phys. Rev. Lett. **114**, 083002 (2015).

[33] Pranjal Bordia, Henrik Lüschen, Sebastian Scherg, Sarang Gopalakrishnan, Michael Knap, Ulrich Schneider, and Immanuel Bloch, "Probing slow relaxation and many-body localization in two-dimensional quasiperiodic systems," Phys. Rev. X **7**, 041047 (2017).

[34] Tarun Grover and Matthew P A Fisher, "Quantum disentangled liquids," Journal of Statistical Mechanics: Theory and Experiment **2014**, P10010 (2014).

[35] N. Y. Yao, C. R. Laumann, J. I. Cirac, M. D. Lukin, and J. E. Moore, "Quasi-many-body localization in translation-invariant systems," Phys. Rev. Lett. **117**, 240601 (2016).

[36] Shankar Iyer, Vadim Oganesyan, Gil Refael, and David A. Huse, "Many-body localization in a quasiperiodic system," Phys. Rev. B **87**, 134202 (2013).

[37] Henrik P. Lüschen, Pranjal Bordia, Sebastian Scherg, Fabien Alet, Ehud Altman, Ulrich Schneider, and Immanuel Bloch, "Observation of slow dynamics near the many-body localization transition in one-dimensional quasiperiodic systems," Phys. Rev. Lett. **119**, 260401 (2017).

[38] Gregory H. Wannier, "Wave functions and effective hamiltonian for bloch electrons in an electric field," Phys. Rev. **117**, 432–439 (1960).

[39] Martin Eckstein and Philipp Werner, "Damping of bloch oscillations in the hubbard model," Phys. Rev. Lett. **107**, 186406 (2011).

[40] D. Nasr Esfahani, L. Covaci, and F. M. Peeters, "Nonlinear response to electric field in extended hubbard models," Phys. Rev. B **90**, 205121 (2014).

[41] Dmitry O. Krimer, Ramaz Khomeriki, and Sergej Flach, "Delocalization and spreading in a nonlinear stark ladder," Phys. Rev. E **80**, 036201 (2009).

[42] P. Pieri and G. C. Strinati, "Derivation of the gross-pitaevskii equation for condensed bosons from the bogoliubov˘de gennes equations for superfluid fermions," Phys. Rev. Lett. **91**, 030401 (2003).

[43] Jean-Claude Garreau, "Quantum simulation of disordered systems with cold atoms," Comptes Rendus Physique **18**, 31 – 46 (2017), prizes of the French Academy of Sciences 2015 / Prix de l'Acadmie des sciences 2015.

[44] L. Sanchez-Palencia, D. Clément, P. Lugan, P. Bouyer, G. V. Shlyapnikov, and A. Aspect, "Anderson localization of expanding bose-einstein condensates in random potentials," Phys. Rev. Lett. **98**, 210401 (2007).

[45] P. Šeba and K. Życzkowski, "Wave chaos in quantized classically nonchaotic systems," Phys. Rev. A **44**, 3457–3465 (1991).

[46] Thomas Guhr, Axel MllerGroeling, and Hans A. Weidenmller, "Random-matrix theories in quantum physics: common concepts," Physics Reports **299**, 189 – 425

(1998).

[47] Jacobs Kurt Rigol Marcos Dunjko Vanja Kennard Harry Yurovsky Vladimir A. Olshanii, Maxim, "An exactly solvable model for the integrabilitychaos transition in rough quantum billiards," Nature Communications **3** (2012), 10.1038/ncomms1653.

[48] David J. Luitz, Nicolas Laflorencie, and Fabien Alet, "Many-body localization edge in the random-field heisenberg chain," Phys. Rev. B **91**, 081103 (2015).

[49] Corentin L. Bertrand and Antonio M. García-García, "Anomalous thouless energy and critical statistics on the metallic side of the many-body localization transition," Phys. Rev. B **94**, 144201 (2016).

[50] Kazue Kudo and Tetsuo Deguchi, "Finite-size scaling with respect to interaction and disorder strength at the many-body localization transition," Phys. Rev. B **97**, 220201 (2018).

[51] A. Chandran, A. Pal, C. R. Laumann, and A. Scardicchio, "Many-body localization beyond eigenstates in all dimensions," Phys. Rev. B **94**, 144203 (2016).

[52] Wojciech De Roeck and Fran çois Huveneers, "Stability and instability towards delocalization in many-body localization systems," Phys. Rev. B **95**, 155129 (2017).

[53] Wojciech De Roeck and John Z. Imbrie, "Many-body localization: stability and instability," Philosophical Transactions of the Royal Society of London A: Mathematical, Physical and Engineering Sciences **375** (2017), 10.1098/rsta.2016.0422.

[54] D.P. Kingma and J. Ba, "Adam: A Method for Stochastic Optimization," ArXiv e-prints (2014), arXiv:1412.6980.